

Study on unloading energy characteristics of limestone in different crossing sections

Yilin Liao¹, Jianfeng Liu^{1*}, Qiangxing Zhang¹, Zhicheng Li², Deng Xu¹ and Anqi Zhu¹

¹State Key Lab of Hydraulics and Mountain River Eng, Editorial Department, 610065 Chengdu, China

²China Railway First Survey and Design Institute Group Co., Ltd, 710043 Xian, China

Abstract. In order to study the energy characteristics of limestone under different initial confining pressures and different unloading rates, based on MTS815 flex test GT rock mechanics test system and acoustic emission (AE) 3D positioning real-time monitoring system, the unloading test and acoustic emission synchronous monitoring of limestone are carried out. The results show that: (1) the pre peak energy process is dominated by energy accumulation, but mainly occurs in the loading stage. The proportion of energy in the unloading stage is basically unchanged, and the proportion of elastic energy is more than 0.9, which fluctuates only before the failure. During the failure, the proportion of energy in the stress drop changes dramatically, and the proportion of elastic energy decreases rapidly to 0. (2) In the coal measure strata, the energy dissipation is the main factor, the dissipation energy and its proportion increase rapidly, while in the front of coal measure strata, the energy release is the main factor, the elastic energy decreases rapidly and the dissipation energy does not increase. (3) The proportion of coal bearing strata in front of coal bearing strata is 0.68 and 0.57 respectively. Unloading elastic energy ratios before coal-bearing strata and coal-bearing strata are 0.824 and 0.876, respectively.

1 Introduction

According to the principle of thermodynamics, in the process of rock deformation and failure, the exchange of material and energy with the outside world constantly takes place. In essence, the fundamental cause of rock deformation and failure is energy driven. In the process of rock deformation and failure, there are both energy input and energy output, and there is always energy conversion in rock, so the process of rock deformation and failure is essentially the process of energy evolution. Because of the influence of excavation rate and initial confining pressure on the mechanical properties of rock, the deformation and failure of rock are different under different excavation conditions, so it is very important to study the influence of unloading rate and initial confining pressure on the mechanical properties of surrounding rock. Based on the construction background of taoziya tunnel, this paper explores the geological conditions of surrounding rock before and in the coal measure strata, and studies the deformation energy characteristics of limestone in these two typical crossing sections.

Liu Xiaoming and Li zhuofen [1] proposed the rock burst damage energy index as the lithologic discrimination method of rock occurrence. Ming Tao [2] uses the continuous surface cover model (CSCM) to simulate the mechanical behavior of rocks. The unloading failure mechanism of hard rock in finite state during unloading is explored. Academician Xie Heping

[3-6] pointed out the energy essence of rock deformation and failure, and believed that the process of rock deformation and failure is driven by energy, which is the result of the combined effect of energy dissipation and energy release. The angle of energy can better reflect the nature of rock deformation and failure. Many scholars have explored the energy evolution characteristics of different rocks under different stress conditions from the perspective of energy. Yang Shengqi [7,8] studied the deformation and energy characteristics of marble under uniaxial and triaxial compression. Zhang Liming [9,10] studied the energy evolution process of limestone and marble under unloading based on the energy perspective. Chen Xuezhong analyzed the stress-strain curve and energy evolution characteristics of marble under high confining pressure unloading. M. C. he [11] uses the release of accumulated energy of acoustic emission to study the mechanism of rapid increase from unloading state to failure state of rock samples. Minke Duan[12] described the cyclic loading and unloading process of surrounding rock by defining permeability enhancement rate (PER), acoustic emission signal change rate and damage variable.

Based on the data of unloading test and theoretical research of surrounding rock at home and abroad, this paper explores the energy evolution law of limestone in two crossing sections under different initial confining pressure and unloading rate based on energy theory, and reveals the influence of stress state on energy release. In this paper, the unloading research of limestone under

* Corresponding author: liujf@scu.edu.cn

three unloading rates and different initial confining pressures under the stable axial pressure unloading path is beneficial to enrich the existing research. The results of this study provide the basis for energy change during excavation and unloading, and provide guidance for the project.

2 Test equipment and test plan

2.1. Test equipment and test pieces

In this test equipment, MTS815 flex test GT rock mechanics test system is used, and PCI - // acoustic emission system is used to synchronously monitor the acoustic emission signal in the process of specimen deformation and failure. The preparation of the test piece shall refer to the provisions of the standard for engineering rock mass test methods (hereinafter referred to as the standard) in GB / T 50266-2013 [13], and the method of dry cutting and turning shall be used for the processing of the test piece. The specimen of unloading triaxial test is a cylindrical specimen with a height of 100mm and a diameter of 50mm (Figure 1)



Fig. 1. Test sample

2.2. Test scheme

2.2.1 Unloading test method of different initial confining pressure

The unloading path is to stabilize the axial pressure and reduce the confining pressure, while maintaining the maximum principal stress unchanged. The unloading rate is 1 MPa / min for reducing confining pressure and 1 MPa / min for increasing deviator stress. The initial confining pressure is 5, 10, 15, 20, 25 and 30MPa respectively.

2.2.2 Unloading test method with different unloading rate

In order to avoid the influence of the maximum principal stress, the unloading path of stabilizing the axial pressure and reducing the confining pressure is adopted in the unloading test. Two groups of different initial confining pressures (10MPa and 30MPa) are set for the unloading test with different unloading rates, and the unloading

rates of each group are set as 2, 3 and 4MPa / min respectively.

3 Experimental results and analysis

3.1. Derivation of energy calculation

Damage evolution. The following describes the energy calculation under unloading conditions. There are three kinds of energy in the process of rock deformation and failure without considering the change of external temperature: the work done by the testing machine to the rock U , Elastic energy stored in rock U_e and Dissipative energy of rock deformation and failure U_d .

According to the conservation of energy:

$$U = U_e + U_d \quad (1)$$

Under the action of three-dimensional stress, from axial loading to failure, the work of the testing machine on the rock is U :

$$U = U_1 + U_2 + U_3 \quad (2)$$

Where U_1 、 U_2 、 U_3 are the work done by the maximum principal stress, the intermediate principal stress and the minimum principal stress respectively.

The relationship between U_1 、 U_2 、 U_3 and stress-strain is as follows:

$$U_i = \int_0^{\varepsilon_i} \sigma_i d\varepsilon_i \quad (3)$$

At the same time, the energy input for the work done by the stress in a certain direction is divided into elastic energy and dissipative energy

$$U_i = U_{ie} + U_{id} \quad (4)$$

Where: U_{ie} and U_{id} are the elastic energy and dissipation energy in a certain direction, U_{ie} can be calculated according to figure 2, and U_{id} is calculated by formula 4.

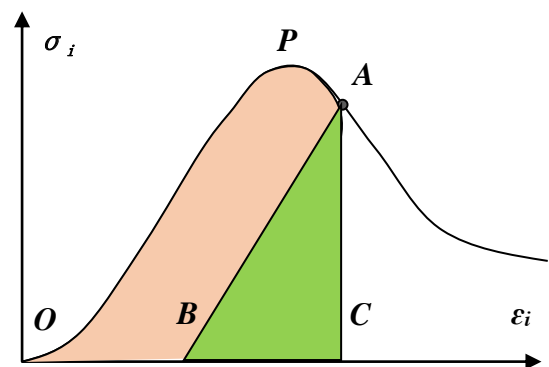


Fig. 2. Calculation of rock deformation and failure energy

In Figure 2, the calculation of U_{ie} is actually based on the assumption that the unloading modulus of elasticity of rock during deformation and failure remains unchanged. Therefore, based on the generalized Hooke's law, U_{ie} can be calculated

General Hooke's law based on linear elasticity is as follows:

$$\begin{cases} \varepsilon_1 = \frac{1}{E} [\sigma_1 - \mu(\sigma_2 + \sigma_3)] \\ \varepsilon_2 = \frac{1}{E} [\sigma_2 - \mu(\sigma_3 + \sigma_1)] \\ \varepsilon_3 = \frac{1}{E} [\sigma_3 - \mu(\sigma_1 + \sigma_2)] \end{cases} \quad (5)$$

Where σ_1 、 σ_2 、 σ_3 are the principal stresses in three directions ε_1 、 ε_2 、 ε_3 are the principal strains in three directions, and are the elastic strains under linear elasticity.

In a certain direction, when the stress and strain meet the linear relationship, according to the relationship between external force work and strain energy which are equal in value, the calculation formula of elastic deformation energy is as follows:

$$U_{ie} = \frac{1}{2} \sigma_i \varepsilon_i \quad (6)$$

$$U_{1e} = \frac{\sigma_1^2 - \mu\sigma_1(\sigma_2 + \sigma_3)}{2E} \quad (7)$$

$$U_{2e} = \frac{\sigma_2^2 - \mu\sigma_2(\sigma_3 + \sigma_1)}{2E} \quad (8)$$

$$U_{3e} = \frac{\sigma_3^2 - \mu\sigma_3(\sigma_1 + \sigma_2)}{2E} \quad (9)$$

Then the elastic energy U_e is

$$U_e = U_{1e} + U_{2e} + U_{3e} \quad (10)$$

According to the conservation of energy, the dissipated energy U_d is:

$$U_d = U - U_e \quad (11)$$

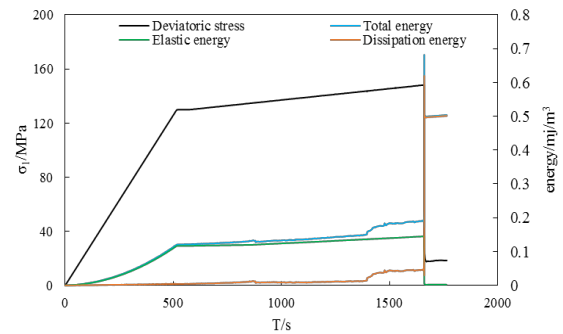
The total energy U is:

$$U = \int_0^{\varepsilon_1} \sigma_1 d\varepsilon_1 + 2 \int_0^{\varepsilon_3} \sigma_3 d\varepsilon_3 \quad (12)$$

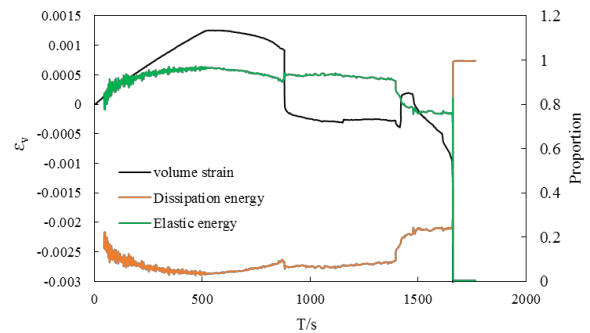
3.2. Influence of initial confining pressure

Taking a typical sample as an example, the energy characteristics of two crossing sections under unloading conditions are discussed. The unloading process of rock can be divided into loading stage, unloading stage and post unloading stage. As shown in Fig. 3 and Fig. 4, in the loading stage, the total energy, elastic energy and dissipated energy increase with the increase of stress. In this stage, the elastic energy is close to the total energy, and the dissipated energy is very small. At the same time, it is noted that in the loading stage, the proportion of elastic energy increases gradually, first fast and then slow, while the proportion of dissipated energy decreases gradually, first fast and then slow, but the two energy proportions change little, and the proportion of elastic energy is 0.9 left Right, and the dissipative energy ratio is about 0.1, which shows that the energy process in the loading stage has energy dissipation but mainly energy accumulation. Compared with the loading stage,

although the total energy, elastic energy and dissipation energy are still increasing in the unloading stage, the growth rate and growth amount are much smaller, because the slow axial loading rate in the unloading stage makes the axial positive work smaller and the negative work in the ring caused by unloading is larger, which makes the energy growth rate and growth amount smaller. In the unloading stage, the energy proportion curve keeps the horizontal energy proportion unchanged, but changes at the end of unloading stage, which is caused by the change of axial deformation before unloading failure. During unloading failure, three kinds of energy change significantly in a short time. For ul1-5, the total energy and dissipation energy rise rapidly while the elastic energy drops rapidly. For ul2-5, the total energy, dissipation energy and elastic energy all drop rapidly. The rapid change of energy corresponds to the rapid change of stress and stress. At the same time, the elastic performance time curve and stress time curve are explained again Consistency of. When unloading failure, corresponding to the rapid change of energy, the proportion of energy also changed significantly. The elastic energy decreased rapidly from a higher proportion to close to 0, while the proportion of dissipation energy increased rapidly to close to 1. The reason for the different change of energy in unloading failure of rock in two crossing sections is the difference of strain curve. In the final analysis, it is the difference of rock mechanical properties in two crossing sections. The rock in front of coal measure stratum is more brittle, even if it is not loaded and depends on its own stored elastic properties, the failure will occur.

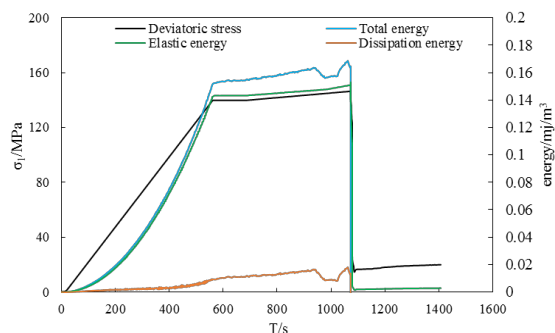


(a) Relationship between deviator stress and energy

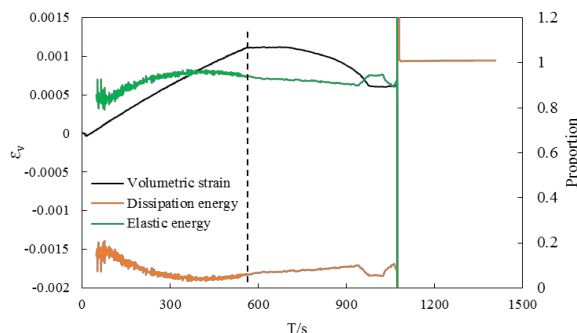


(b) Relationship between volume strain and energy proportion

Fig. 3. Energy evolution characteristics of UL1-5



(a) Relationship between deviator stress and energy



(b) Relationship between volume strain and energy proportion

Fig. 4. Energy evolution characteristics of UL2-5

The unloading failure of rock occurs at the peak stress. After the peak stress, the total energy, elastic energy and dissipation energy all increase abruptly. Therefore, the total energy, elastic energy and dissipation energy at the peak stress can explain the energy characteristics of unloading failure. Table 1 shows the total energy, elastic energy and dissipative energy at the peak stress before triaxial unloading failure of the rock in two crossing sections.

Table 1. Peak stress point energy of two crossing sections under unloading condition.

Traversing section	Sample number	σ_3 / MPa	σ_{max} / (MPa)	U / (MJ/m ³)	U_e / (MJ/m ³)	U_d / (MJ/m ³)
In coal measures	UL1-5	5	148.11	0.171	0.145	0.027
	UL1-10	10	157.22	0.192	0.174	0.018
	UL1-15	15	179.03	0.259	0.195	0.064
	UL1-20	20	198.34	0.310	0.249	0.061
	UL1-25	25	222.32	0.405	0.340	0.065
	UL1-30	30	243.36	0.504	0.404	0.100
Before coal measures	UL2-5	5	146.44	0.165	0.153	0.013
	UL2-10	10	157.17	0.193	0.165	0.028
	UL2-15	15	176.08	0.278	0.163	0.115
	UL2-20	20	188.08	0.281	0.257	0.023
	UL2-25	25	197.67	0.384	0.322	0.044
	UL2-30	30	216.08	0.360	0.287	0.073

It can be seen from table 1, figure 5 and Figure 6 that the peak stress increases with the increase of initial confining pressure during unloading failure of rock in the two crossing sections; although there are some data with large deviation, the total energy, elastic energy and dissipation energy all increase with the increase of confining pressure. Excluding individual data, the total energy, elastic energy and dissipation energy at the peak stress have good linear relationship with the initial confining pressure. Due to the expansion of tensile crack under unloading condition, the rock sliding without friction makes the stress required for failure smaller. Another explanation is that under unloading condition, the circumferential negative work is larger and the total energy is smaller.

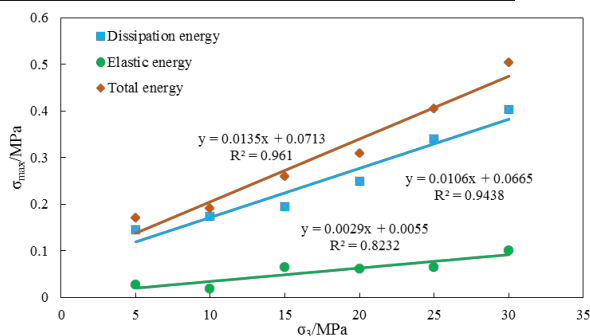


Fig. 5. Relationship between UL1 peak point energy and confining pressure

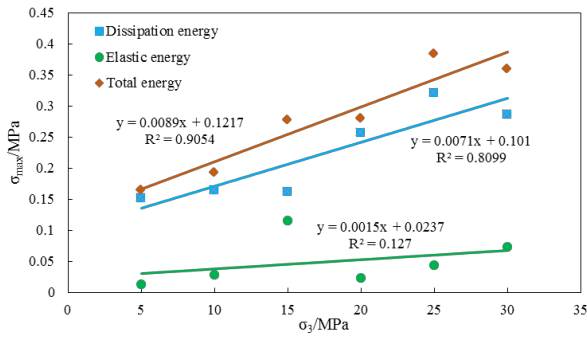


Fig. 6. Relationship between UL2 peak point energy and confining pressure

3.3. Effect of unloading rate

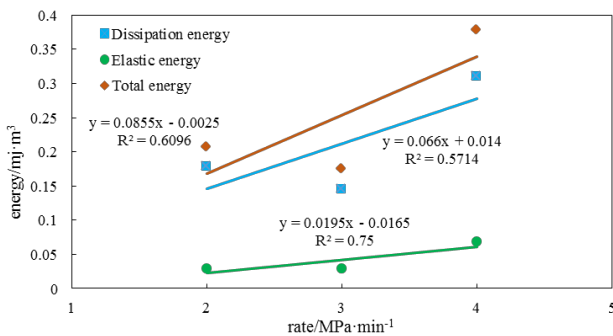
Limited by sampling, only the samples in front of coal measure strata are tested for unloading at different unloading rates under 10MPa and 30MPa confining pressure. The unloading confining pressure rate does not change the form of axial energy and total energy curve, but changes the changing rate of curve at different stages. In order to explore the influence of unloading rate on unloading energy quantitatively, table 2 shows 10MPa

and 30MPa of samples in front of coal measure strata Energy at peak stress at three different unloading rates at 30MPa.

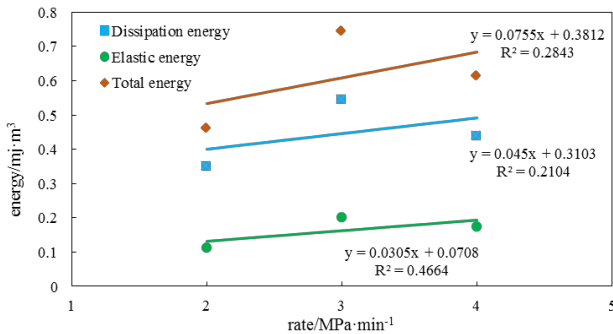
From table 2, for 10MPa initial confining pressure, with the increase of unloading rate, the peak stress increases gradually, while for 30MPa initial, with the increase of unloading rate, the peak stress increase trend is not obvious. But on the whole, the unloading strength of 30MPa is higher than 10MPa. The energy at the unloading peak stress of 30MPa initial confining pressure is also greater than 10MPa overall. The relationship between the total energy, elastic energy and dissipative energy under the two confining pressures and the rate of pressure relief can be seen more intuitively through Figure 7. It can be seen from Figure 7 that the initial rule of 10MPa and 30MPa is the same, and the total energy, elastic energy and dissipation energy all increase with the increase of unloading rate. Figure 8 shows the relationship between elastic energy ratio and unloading rate under two confining pressures. Figure 8 shows that the elastic energy ratio decreases with the increase of unloading rate.

Table 2. Peak stress point energy of two crossing sections under unloading condition.

Sample number	$\sigma_3/$ (MPa)	$V/$ (MPa/min)	$\sigma_{max}/$ (MPa)	$U/$ (MJ/m ³)	$U_e/$ (MJ/m ³)	$U_d/$ (MJ/m ³)
UL2-10-2-2	10	2	143.50	0.208	0.179	0.029
UL2-10-3-3	10	3	147.02	0.175	0.146	0.029
UL2-10-4-4	10	4	150.44	0.379	0.311	0.068
UL2-30-2-2	30	2	234.82	0.463	0.350	0.113
UL2-30-3-3	30	3	219.01	0.746	0.546	0.200
UL2-30-4-4	30	4	229.24	0.614	0.440	0.174



(a) $\sigma_3=10\text{MPa}$



(b) $\sigma_3=30\text{MPa}$

Fig. 7. Relationship between peak stress point energy and unloading rate at different unloading rates

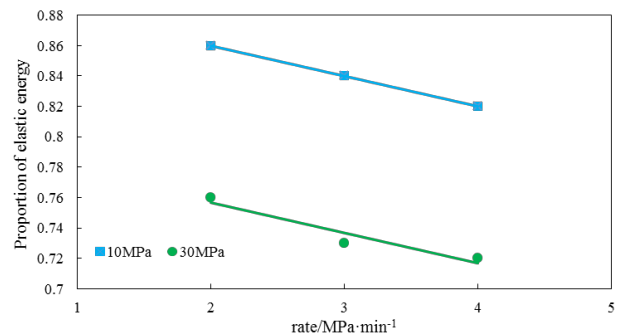


Fig. 8. Energy characteristics of peak stress points at different unloading rates

4 Conclusion

1) Under the unloading condition, the energy evolution stage is consistent with the deformation stage. The energy process before the peak is mainly energy accumulation, but mainly occurs in the loading stage. The proportion of energy in the unloading stage is basically unchanged, only fluctuates before the failure.

2) The elastic energy ratio is more than 0.9, and only fluctuates before the failure. During the failure, the stress drops and the energy ratio changes dramatically, and the elastic energy ratio drops rapidly to 0.

3) In the coal measure strata, the main energy dissipation is energy dissipation, and the total energy and dissipation energy rise sharply. In front of the coal measure strata, the energy is mainly released, and the total energy and dissipation energy drop sharply.

4) When the rock in coal measure strata is destroyed, the energy increases rapidly with the increase of confining pressure.

References

1. Liu Xiaoming, Li Zhuofen. Damage mechanics analysis and rock burst damage energy index of brittle rock [J]. *Journal of rock mechanics and engineering*, 1997 (02): 45-52
2. Ming Tao, Xibing Li, Di Yuan Li. Rock failure induced by dynamic unloading under 3D stress state [J]. *Theoretical and Applied Fracture Mechanics*, 2013, 65
3. Xie Heping, Ju Yang, Li Liyun, et al. Energy mechanism of rock deformation and failure process [J]. *Journal of rock mechanics and engineering*, 2008 (09): 1729-1740
4. Xie Heping, Ju Yang, Li Liyun. Rock strength and overall failure criterion based on energy dissipation and release principle [J]. *Journal of rock mechanics and engineering*, 2005 (17): 3003-3010
5. Xie Heping, Peng Ruidong, Ju Yang. Analysis of energy dissipation in the process of rock deformation and failure [J]. *Journal of rock mechanics and engineering*, 2004 (21): 3565-3570
6. Xie Heping, Peng Ruidong, Ju Yang, Zhou Hongwei. Energy analysis of rock failure [J]. *Journal of rock mechanics and engineering*, 2005 (15): 2603-2608
7. Yang Shengqi, Xu Weiya, Su Chengdong. Study on failure and energy characteristics of rock samples under uniaxial compression [J]. *Journal of solid mechanics*, 2006 (02): 213-216
8. Yang Shengqi, Xu Weiya, Su Chengdong. Study on triaxial compression failure and energy characteristics of marble [J]. *Engineering mechanics*, 2007 (01): 136-142
9. Zhang Liming, Gao Xun, Wang Zaiquan. Experimental study on energy consumption of limestone under loading and unloading [J]. *Geotechnical mechanics*, 2013, 34 (11): 3071-3076
10. High speed, Zhang Liming, Wang Zaiquan, et al. Study on deformation and energy characteristics of marble under unloading [J]. *Journal of rock mechanics and engineering*, 2014, 33 (S1): 2808-2813
11. M.C. He, J.L. Miao, J.L. Feng. Rock burst process of limestone and its acoustic emission characteristics under true-triaxial unloading conditions [J]. *International Journal of Rock Mechanics and Mining Sciences*, 2009, 47(2)
12. Yi Luo. Mechanical Properties and Energy Analysis of Rock under Different Unloading Confining Pressures [C]. Institute of Management Science and Industrial Engineering. Proceedings of 2019 6th International Conference on Machinery, Mechanics, Materials, and Computer Engineering (MMMCE 2019). Institute of Management Science and Industrial Engineering: (Computer Science and Electronic Technology International Society), 2019: 205-210
13. Former Ministry of electric power industry of the people's Republic of China. GB / T 50266-2013 engineering rock mass test method standard [S]. Beijing: China Planning Press, 2013